17th World Conference on Earthquake Engineering, 17WCEE
Sendai, Japan - September 13th to 18th 2020

Shear Strength of Post-installed Anchor and Cylindrical Shear-key in Seismic Reinforcement Joints

T. Abe[(1)], K. Sakamoto[(2)], T. Hiwatashi[(3)], Y. Takase[(4)], K. Katori[(5)]

[(1)] ***Chief, Seismic Solution Department, TOBISHIMA Corporation, Takahide_Abe@tobishima.co.jp***
[(2)] ***Chief, Seismic Solution Department, TOBISHIMA Corporation, Keita_Sakamoto@tobishima.co.jp***
[(3)] ***Senior Researcher, Research and Develop Center, TOA Corporation, t_hiwatashi@toa-const.co.jp***
[(4)] ***Associate Professor, College of Design and Manufacture Technology, Muroran Institute of Technology, y.takase@mmm.muroran-it.ac.jp***
[(5)] ***Professor, Department of Architecture, Faculty of Science & Engineering, Toyo University, katori@toyo.jp***

Abstract

In seismic retrofitting of existing structures, roughening by chipping and post-installed anchors are often used at joints that join reinforcing members such as steel beam braces or damping braces with the existing frame. As interlocking and bearing resistances from roughening have high rigidity and can contribute to shear strength, it is highly useful to reflect these in the design of joints, and it can be expected that shear displacement of the interface between the existing frame and the reinforcements will be kept small. In other words, it is possible to control the shear displacement of the joint surface using a mechanical model that combines both the dowel action of post-installed anchors and the local interlocking and bearing resistances due to roughening, which can enhance the effect of reinforcing members during earthquakes.

The authors have proposed a cylindrical shear-key as a joining technique that replaces roughening in consideration of the construction environment. This construction method has the characteristic that the vibration, noise, and dust generation can be considerably reduced compared to roughening because the shape of the recess is formed in the existing frame using a core drill. Furthermore, since the shape of the recess is equalized regardless of the workmanship, quantitative evaluation of the shear strength is possible. In addition, when this cylindrical shear-key is used on the joint surface instead of roughening, as described above, it is used in combination with a post-installed anchor in the same manner as roughening to suppress the shear displacement of the joint surface and to considerably increase shear strength.

The authors have conducted a shear test where a cylindrical shear-key and a post-installed anchor were combined. From the results of the experiment, they estimated the stress state and mechanical behavior due to axial stress of the joint, and proposed a shear strength formula during combined use that reflects these effects.

Keywords: Seismic retrofitting, Post-installed anchor, Cylindrical shear-key, Shear strength

1. Introduction

In seismic retrofitting of existing structures, the joints that connect reinforcing members such as steel beam braces and damping braces with the existing frame are often roughened by chipping (herein simply referred to as roughened) and post-installed adhesive anchors (herein termed post-installed anchors). Interlocking and bearing resistances have high rigidity due to roughening [1], which can contribute to shear strength; therefore, it is extremely useful to appropriately evaluate and reflect them in joint design; it can be expected that the shear displacement at the interface between the existing frame and reinforcing members is kept small. In other words, it is possible to control the shear displacement of the joint surface by designing for the combined use of interlocking and bearing resistances due to roughening, which can enhance the effect of reinforcing members during earthquakes.

Considering the construction environment, the authors have proposed a cylindrical shear-key [2] as a joining technique to replace roughening. This construction method is characterized by a considerable reduction in the vibration, noise and dust generation compared to roughening because the shape of the recess is formed in the existing frame using a core drill. Furthermore, as the shape of the recess is uniform regardless of workers' skill, quantitative evaluation of the shear strength is possible. In addition, when this cylindrical shear-key is used on the joint surface instead of roughening, as previously described, it is used in combination with post-installed anchors in the same manner as roughening to suppress shear displacement of the joint surface and to considerably increase shear strength.

The authors have constructed and reported on a precise dynamic model [2],[3] in which the bearing resistance of a cylindrical shear-key and the dowel resistance of a post-installed anchor were used independently (herein termed "individual use"). When used in combination (herein termed "combined use"), their mechanical behaviors need to be assessed, as they are notably different.

Thus, in this study, a shear test was first performed, combining the use of a cylindrical shear-key and a post-installed anchor. The stress state and mechanical behavior due to axial stress on the joint surface was estimated from the results of the experiment, with the purpose of proposing a shear strength formula for combined use that reflects these effects.

2. Mechanical behavior assuming a cylindrical shear-key and a post-installed anchor

Figure 1 shows the concept of the assumed shear resistance elements and mechanical behavior of the joints. The shear resistance elements of the joint surface are considered to be bearing resistance from the cylindrical shear-key, the dowel action from the post-installed anchor, and the friction and bonding resistances of the joint surface. In this experiment, grease was applied to the parts other than the cylindrical shear-key to minimize frictional and bonding resistances generated on the joint surfaces. As the existing concrete and reinforcement member grout separated accompanying the increase in shear displacement on the joint surface, δ_H, described later, in this study we focused only on bearing resistance and dowel action.

Owing to the design of the joint, δ_H is often suppressed to be 2 mm or less [4]; focusing on δ_H up to 2 mm, when it reaches maximum shear force (corresponding to δ_{peak} in Figure 1(b)), Q_{max} is approximately 0.2 mm, Q_{max} is generally maintained and the load decreases. The shear displacement at which this load loss begins is defined as δ_{max}. As shown in Figure 1(c), the mechanical model based on the dowel action of the post-installed anchor is constructed using the reaction force coefficient from the elastic bearing beam equation [3]. As δ_H increases up to δ_H =2 mm, shear force Q tends to gradually increase, accompanied by a gradual decrease in rigidity.

From the aforementioned, the different mechanical behaviors of the cylindrical shear-key and the post-installed anchor need to be considered when they are used in combination in the shear strength analysis.

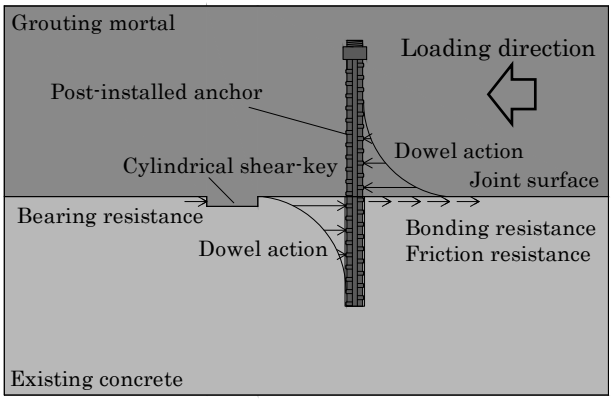

(a) Image of shear resistance elements

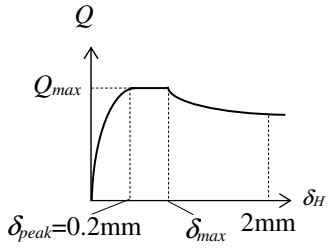

(b) Mechanical model of cylindrical shear-key

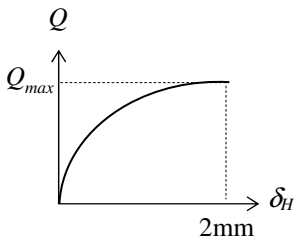

(c) Mechanical model of post-installed anchor

Figure 1 Concept of the assumed shear resistance elements and mechanical behavior of the joints

3. OUTLINE OF SHEAR LOADING TEST

3.1 Test parameters

Table 1 shows the experiment parameters and the results of materials tests. The main parameters were obtained from a specimen in which only a post-installed anchor was fitted (herein termed series A), and a specimen with both, a post-installed anchor and cylindrical shear-keys (herein termed series AS).

The variable factor in series A was the strength of the concrete in existing parts, ${}_C\sigma_B$. In addition, generally, ${}_C\sigma_B$ for buildings requiring seismic retrofitting is between 13.5 – 30 N/mm^2, and the targets are set at three levels in this range when pouring concrete. The diameter and steel grades for the anchor bolts were set as D16 and SD345, commonly used for seismic reinforcement. Regarding the average compression stress of the joint surface σ_0, it was set to 0.48 N/mm^2, based on a previous study [5] using a steel shear-key for

joints as a method of internal reinforcement that reported a change of about 0.4 N/mm^2 in regions where shear deformation of the joint surface was less than 1 mm. Moreover, as shown in the following equation, σ_0 is obtained by the ratio of the axial force N and the area of the surface joint, A.

$$\sigma_0 = N/A \tag{1}$$

The variables in series AS were σ_0 and ${}_C\sigma_B$. σ_0 was set to 0.48 N/mm^2 and 0.95 N/mm^2, and to enable the comparison with series A, ${}_C\sigma_B$ was also taken as 3 levels, where σ_0=0.48 N/mm^2, and 2 levels where σ_0 =0.95 N/mm^2. The authors published [6] shear strength formulas for cylindrical shear-keys of diameters in the range of R=40 – 60 mm; thus, R =52 mm was considered as the standard of this range. Moreover, the type of failure of the cylindrical shear-key differs depending on the width-to-height ratio (herein termed R/t), which is the ratio of R and the height of the cylindrical shear-key, t. R/t was set to be R/t=10 in this study, assuming a bearing failure. Note that the diameter and steel grade of the anchor bolts was the same as in series A.

Table 1 Test parameters and material test results

No.	σ_0	Existing concrete		Grouting mortal		Cylindrical shear-key		Anchor bolt		
		${}_C\sigma_B$	E_C	${}_G\sigma_B$	E_G	R	R/t	d_a	σ_y	E_S
A16-LL1	0.48	14.5	22.1	57.3	24.8	-	-	D16	379	181
A16-LM1		17.8	25.7	69.4	25.7				381	189
A16-LH1		29.9	26.3	57.3	24.8				369	196
A16S52-10LL1,2	0.48	14.5	22.1	57.3	25.8	52	10.4	D16	379	181
A16S52-10LM1		21.7	26.5	56.6	26.7					
A16S52-10LH1,2		32.9	27.7	57.3	25.8					
A16S52-10ML1,2	0.95	14.5	22.1	57.3	25.8					
A16S52-10MM1		21.7	26.5	56.6	26.7					

${}_C\sigma_B$: Concrete compressive strength, E_C :Concrete elastic modulus,
${}_G\sigma_B$: Grouting mortal compressive strength, E_G :Grouting mortal elastic modulus,
R : Diameter of cylindrical shear-key, R/t : Width to height ratio,
σ_y : Anchor bolt yield strength, E_S : Anchor bolt elastic modulus, d_a: Diameter of anchor bolt

Explanatory notes of specimen No. : A 16 S 52 - 10 L L 2
Post-installed anchor / R / R/t / σ_0 / ${}_C\sigma_B$ / Branch number
Diameter of anchor bolt / Cylindrical shear-key
σ_0 L : 0.48N/mm^2, M : 0.95N/mm^2
${}_C\sigma_B$ L : Low level, M : Middle level, H : High level

3.2 Specimen dimensions

Figure 2 shows the dimensions of the test specimens. In series A, the post-installed anchor was fitted in a double arrangement, with pitch of 150 mm and gauge of 85 mm. For the installation of the post-installed anchor, after drilling with a wet-core drill, flat-cut anchor bolts were fixed using epoxy adhesive. The effective embedded depth of the post-installed anchor, L_e, was set to 7 times the diameter (d_a) of the anchor bolt at 7d_a. In series AS, the pitch, gauge, and arrangement of the cylindrical shear-keys were the same as those of the post-installed anchor bolts.

The reinforcement members of the test specimen were grouted to simulate the joint used for seismic retrofitting, and their height and width were both set to 200 mm, the general cross-sectional dimensions of seismic reinforcements. In addition, as the existing concrete simulates the beams of an existing building,

their width and height were set to 400 and 200 mm, respectively, and their length to 750 mm, larger than the dimensions of the reinforcement grout.

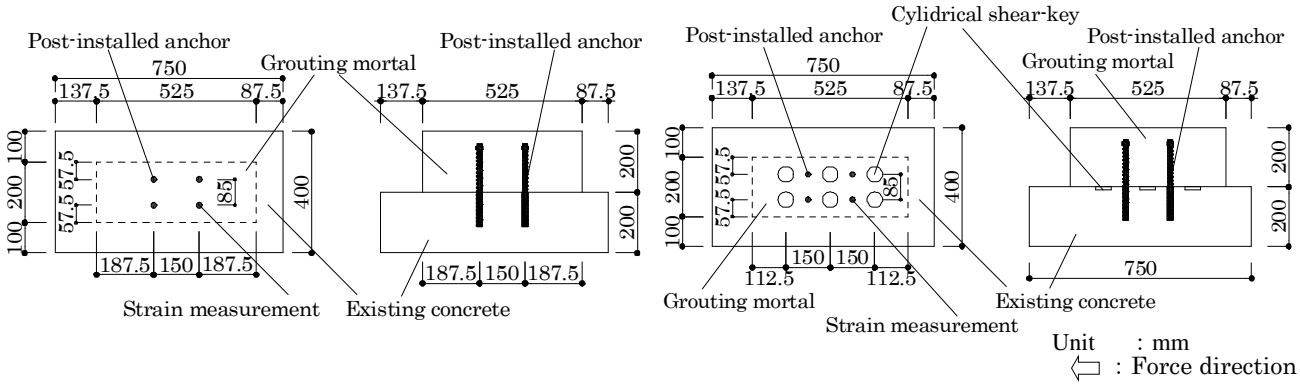

(a) Series A (b) Series AS

Figure 2 Dimensions of specimen

3.3 Loading and measurement

Figure 3 shows the loading device. Constant load control, using an actuator with maximum load of 200 kN, and unidirectional monotonic loading, using a hydraulic jack of maximum load 500 kN, were utilized in the axial and horizontal directions. As shown in the figure, a bi-directional roller bearing was used for the thick steel plate subjected to pressurization to minimize the frictional resistance caused by the load device. A rubber sheet was fitted between the thick steel plate subjected to pressurization and the reinforcement grout, enabling even distribution of the axial force throughout the specimen.

The displacement at the joint surface δ_H, and the separation distance between the existing concrete and the reinforcement grout δ_V were measured. High sensitivity displacement meters were placed on the existing concrete in two locations, and the average of the measured values was used for δ_H and δ_V.

Figures 3 and 4 show the positions of the post-installed anchor after strain measurement and the strain measurement, respectively. To calculate the elastic bending moment and elastic axial force of the anchor bolt from the results of the experiment, strain was measured at the front and rear of the loading direction.

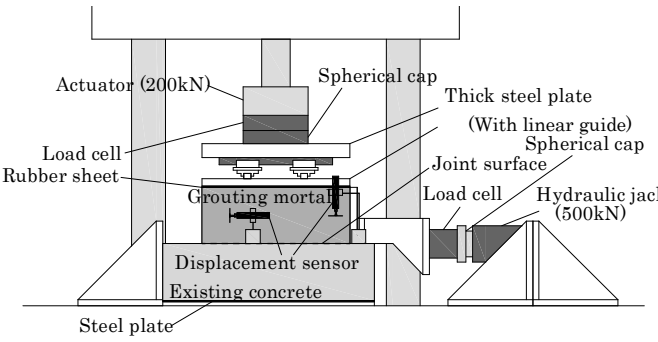

Figure 3 Loading equipment of shear loading test

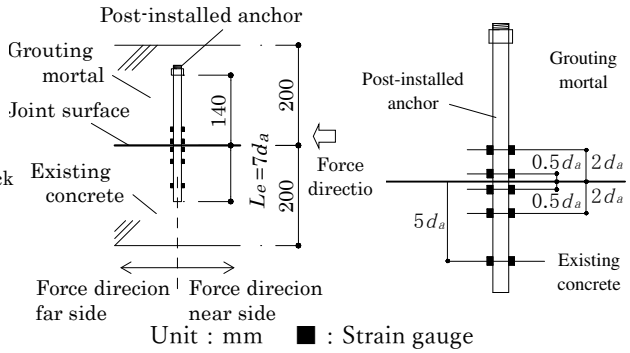

Figure 4 Strain measurement position

4. MECHANICAL BEHAVOR OF JOINT

4.1 Mechanical model of single

Shear force ${}_{\delta}Q_a$ for shear displacement δ_H using only a post-installed anchor, shown in Figure 1(b), is reported by the authors in reference [3]. Moreover, the mechanical behavior in which only the cylindrical shear-key exposed in Figure 1(c) is used is represented by the mechanical model shown in Figure 5 [2], and this model consists of three regions: gradually increasing, fixed and reducing load regions. For each region, shear force ${}_{\delta}Q_{sky}$ when the shear displacement of bearing failure δ_H while using a cylindrical shear-key is given by the following equations:

$$\frac{{}_{\delta}Q_{sky}}{{}_{b}Q_{sky}} = 6.75\left(e^{-0.812\left(\frac{\delta_H}{\delta_{peak}}\right)} - e^{-1.218\left(\frac{\delta_H}{\delta_{peak}}\right)}\right) \qquad (0 \le \delta_H/\delta_{max} \le \delta_{peak}/\delta_{max}) \tag{2}$$

$$\frac{{}_{\delta}Q_{sky}}{{}_{b}Q_{sky}} = 1 \qquad (\delta_{peak}/\delta_{max} \le \delta_H/\delta_{max} \le 1) \tag{3}$$

$$\frac{{}_{\delta}Q_{sky}}{{}_{b}Q_{sky}} = {}_{b}\gamma \cdot ln(\delta_H/\delta_{max}) + 1 \qquad (1 \le \delta_H/\delta_{max} \le 5/\delta_{max}) \tag{4}$$

where, ${}_{b}Q_{sky}$ is the shear strength of the bearing-failure type cylindrical shear-key, δ_{peak} is δ_H when ${}_{b}Q_{sky}$ is reached, and δ_{max} is δ_H at the end of the fixed-load region. Note that δ_{peak} is 0.2 mm in reference [2]. Moreover, ${}_{b}\gamma$ is a function that expresses the decrease in ${}_{\delta}Q_{sky}$ in the bearing-failure type load loss region; δ_{max} and ${}_{b}\gamma$ are as follows:

$$\delta_{max} = 0.42\sigma_0 \tag{5}$$

$${}_{b}\gamma = {}_{b}A \cdot ln(\sigma_0') + {}_{b}B \tag{6}$$

$$\sigma_0' = N/{}_{p}A_{sky} \tag{7}$$

where, ${}_{b}A$ (=0.052) and ${}_{b}B$ (=-0.229) are coefficients; ${}_{p}A_{sky}$ is the horizontal projected area of the arranged cylindrical shear-keys, and σ_0' is the average compressive stress generated in the cylindrical shear-keys.

${}_{b}Q_{sky}$ is calculated using Equation (8), multiplying shear strength per bearing-failure type cylindrical shear-key, ${}_{b}q_{sky}$, by the number of cylindrical shear-keys positioned on the joint surface, n_{sky}; ${}_{b}q_{sky}$ is calculated according to Equations (9)-(14).

$${}_{b}Q_{sky} = n_{sky} \cdot {}_{b}q_{sky} \tag{8}$$

$${}_{b}q_{sky} = A_{sky} \cdot \sigma_{cs} \tag{9}$$

$$A_{sky} = \frac{\pi \cdot R \cdot t}{2} \tag{10}$$

$$\sigma_{cs} = C_C \cdot C_N \cdot C_R \cdot \bar{\sigma}_{cs} \tag{11}$$

$$C_C = \frac{0.552\ {}_{C}\sigma_B + 44.2}{56.0} \qquad (10.3 \le {}_{C}\sigma_B \le 32.9\mathrm{N/mm^2}) \tag{12}$$

$$C_N = \frac{39.1\sigma_0 + 34.8}{71.9} \qquad (0.48 \le \sigma_0 \le 1.43\mathrm{N/mm^2}) \tag{13}$$

$$C_R = \frac{-1.32R + 123}{56.0} \qquad (40 \le R \le 60\mathrm{mm}) \tag{14}$$

where, A_{sky} is the area subjected to pressure, σ_{cs} is the shear direction component of average bearing stress σ_c during ${}_bq_{sky}$; C_C, C_N, C_R are the correction coefficients for ${}_C\sigma_B$, σ_0 and R, respectively, and $\overline{\sigma_{cs}}$ (=75.3N/mm^2) is the average bearing stress.

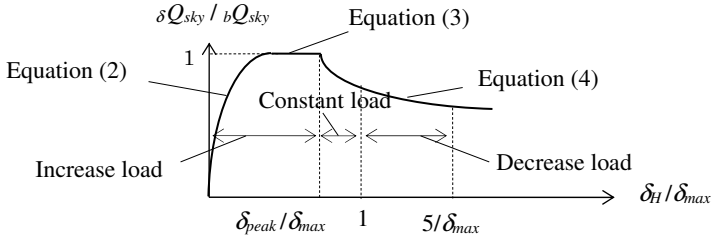

Figure 5 Mechanical model of cylindrical shear-key under individual use

4.2 Consideration on combined mechanical behavior

Figure 6 shows the δ_V-δ_H relationship. In series A, δ_V is about 1/10 of δ_H, but in series AS it generally ranges from 1/10 to 1/2 of δ_H. In other words, it is understood that under combined use, δ_V increases due to the effects of the cylindrical shear-key. This suggests that a series AS anchor bolt with a large δ_V has a higher tensile force than in series A. Takase et al. [7] quantified and published the phenomenon in which shearing force decreases as tensile force generated by the anchor bolts increases as a result of a shear test using the tensile force generated in the anchor bolt. Considering this tendency, it is inferred that shear force ${}^C{}_\delta Q_a$ at the time of shear displacement δ_H borne by the post-installed anchor under combined use is smaller than ${}_\delta Q_a$ under individual use. Figure 7 shows the concept of the stress state at the joint surface under combined use. It is assumed that the axial force generated in the cylindrical shear-keys N_{sky} increases because of the balance between axial stress T generated in the anchor bolt due to δ_V.

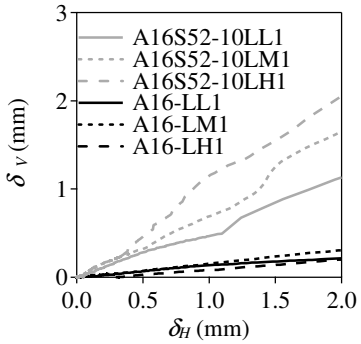

Figure 6 $\delta_V - \delta_H$ relationship

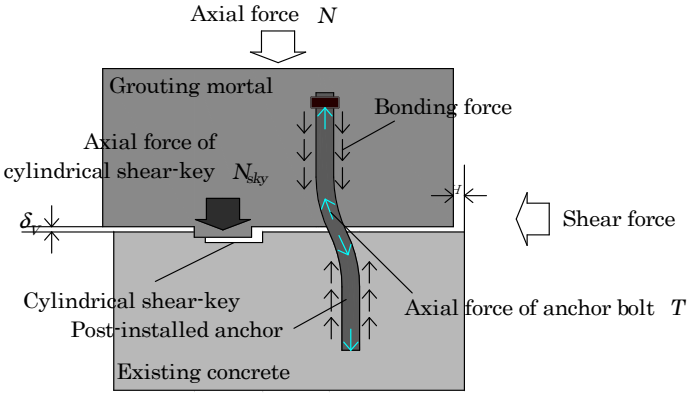

Figure 7 The concept of the stress state at the joint surface under combined use

4.3 Estimation of axial stress occur at joint surface

As shown in Figure 7, from the balance of the vertical component of T (the tensile axial force of the anchor bolt is positive) and ${}_vN_a$ (the direction of compressive axial force on the joint surface), and the balance stress from N and N_{sky}, N_{sky} is calculated using the following equation:

$$N_{sky} = N - {}_vN_a \tag{15}$$

As ${}_vN_a$ is the vertical component of T, it can be calculated from the following equation using the

relationship between δ_H and δ_V.

$$ {}_vN_a = -T \cdot n_a \cdot \sin(\tan^{-1}\left(\frac{\delta_V}{\delta_H}\right)) \tag{16}$$

From the values obtained from stresses of anchor bolt strain, σ_1 and σ_2, T within the elastic range and bending moment M are calculated using Equations (17) and (18), respectively, while stress at the time the anchor bolt yields from T and M, σ_y, is calculated using Equation (19).

$$T = \frac{(\sigma_1 + \sigma_2)}{2} \cdot \frac{\pi {d_a}^2}{4} \tag{17}$$

$$M = \frac{(\sigma_1 - \sigma_2)}{2} \cdot \frac{\pi {d_a}^3}{32} \tag{18}$$

$$\sigma_y = \frac{M}{Z_a} + \frac{T}{A_e} \tag{19}$$

where, Z_a and A_e are the section-modulus and the sectional area of the anchor bolt, respectively.

From Equations (17) and (18), Figures 8 and 9 show an example of the M-distribution of the anchor bolt within the elastic range when δ_H =0.25 mm and an example of the T-distribution. As expected, M presents a smaller value in series AS than in series A, while T presents a larger value in series AS than in series A.

From Figure 8, it is observed that the depth of existing concrete reaching σ_y, l_e, is in the range l_e =0.5d_a to l_e =2d_a; thus, in this study we used M and T values of l_e =2d_a, which have relatively small variations, and determined that the anchor bolt reached σ_y. Moreover, to estimate ${}_vN_a$, it was appropriate to use a value of T as close as possible to the joint surface, and so ${}_vN_a$ was calculated using the average of the T values of the existing concrete side, l_e =0.5d_a and the reinforcement grout side l_e =0.5d_a. Considering the value of the ratio of ${}_vN_a$ and A as the average compressive stress on the joint surface due to ${}_vN_a$, ${}_a\sigma_0$, we calculated ${}_a\sigma_0$, as follows:

$$ {}_a\sigma_0 = {}_vN_a / A \tag{20}$$

From ${}_a\sigma_0$ and the anchor bolt tension, we observe the T/T_a relationship, which is the ratio of T to yield load T_a(=$\sigma_y \times A_e$). Figure 10 shows the ${}_a\sigma_0$-T/T_a relationship. From the figure, the T/T_a average value is 0.18 and 0.39 in series A and AS, respectively. Although variation was observed, the average value of ${}_a\sigma_0$ was -0.56 and -0.05 N/mm^2 in series AS and A, respectively. Thus, it is seen that the ${}_a\sigma_0$ value is very small in Series A, but sufficiently large in series AS to affect shear force. In addition, shear displacement δ_{Hy} was 0.53 mm when it reached σ_y, calculated using Equation (19).

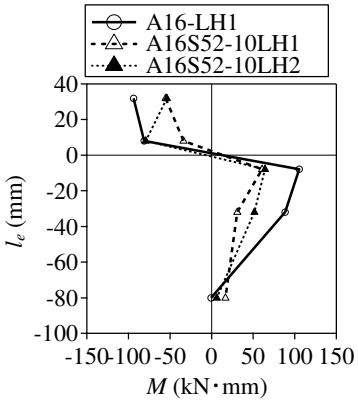

Figure 8 M-distribution

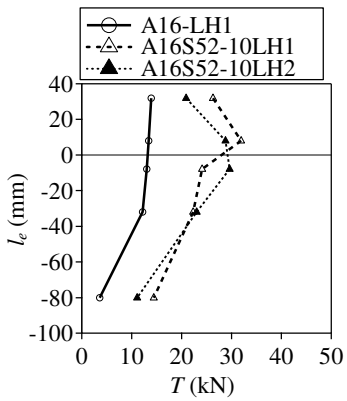

Figure 9 T-distribution

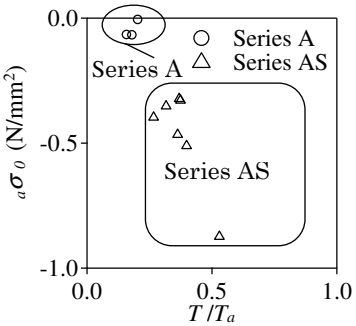

Figure 10 ${}_a\sigma_0$ — T/T_a relations

5. Shear Strength Equation for Combined Use

5.1 Shear strength formula

In this study, shear force when δ_H =2 mm is considered the shear strength. Assuming that the shear force of the joint surface ${}^{C}{}_{2mm}Q$ is cumulative for the deformation of ${}^{C}{}_{2mm}Q_a$ and ${}^{C}{}_{2mm}Q_{sky}$, it can be expressed as:

$$ {}^{C}{}_{\delta}Q = {}^{C}{}_{\delta}Q_a + {}^{C}{}_{\delta}Q_{sky} \tag{21} $$

First, to examine the shear strength of the post-installed anchor under combined use, we estimated the value of the reduction rate of shear strength borne by the post-installed anchor; ${}^{C}{}_{2mm}Q_a / {}_{2mm}Q_a$. Takase et al. [7] applied the following equation, which is generally used in the design of structural members subjected to the combination of tensile and shear stresses.

$$ \left(\frac{T}{T_a}\right)^{{}^{C}\alpha} + \left(\frac{Q_y}{Q_a}\right)^{{}^{C}\alpha} = 1 \tag{22} $$

where, Q_a is the shear strength of the post-installed anchor, Q_y is the shear force borne by the post-installed anchor under shearing displacement δ_{Hy}, and ${}^{C}\alpha$ is the coefficient of T/T_a and Q_y/Q_a.

The average value of δ_{Hy} in series AS is 0.53 mm; as ${}^{C}\alpha$ is within 0.75 - 1.00 [7], when ${}^{C}\alpha$ = 0.75 and 1.00, Q_y/Q_a is calculated using Equation (22). The Q_y/Q_a in series AS is in the range of 0.62 to 0.74 times that of series A. In this study, we attempted to examine the condition in which ${}^{C}{}_{\delta}Q_a$=0.7${}_{\delta}Q_a$.

In sequence, we described the shear strength of the cylindrical shear-key. N_{sky} at δ_{Hy} is calculated from Equation (15), and the average compressive stresses at the joint surface and generated in the cylindrical shear-key under combined use, ${}^{C}\sigma_0$ and ${}^{C}\sigma_0$' , respectively, are found using the following equations:

$$ {}^{C}\sigma_0 = \frac{N - {}_{v}N_A}{A} = \sigma_0 - {}_{a}\sigma_0 \tag{23} $$

$$ {}^{C}\sigma_0' = \frac{N_{sky}}{{}_{p}A_{sky}} = \frac{\left(N - {}_{a}\sigma_0 \cdot A\right)}{{}_{p}A_{sky}} \tag{24} $$

From ${}_{a}\sigma_0$ =-0.56 N/mm^2, obtained in Section 4.3, the value used for design was ${}_{a}\sigma_0$ =-0.60 N/mm^2. In Equations (5) - (7) and (13), σ_0 is substituted for ${}^{C}\sigma_0$ and σ_0' for ${}^{C}\sigma_0$'. As a result, ${}^{C}{}_{2mm}Q_{sky}$, ${}^{C}{}_{\delta}Q_{sky}$ at δ_H =2 mm, is 1.26 times that of ${}_{2mm}Q_{sky}$ (σ_0=0.48 N/mm^2) – 1.44(σ_0= 1.43 N/mm^2), and ${}_{2mm}Q_{sky}$ shifts to 0.64(σ_0=0.48 N/mm^2) – 0.88(σ_0=1.43 N/mm^2) that of ${}_{b}Q_{sky}$. From the aforementioned, when ${}^{C}{}_{2mm}Q_{sky} / {}_{b}Q_{sky}$ is complemented with a linear function of σ_0 within the range $0.48 \leqq \sigma_0 \leqq 1.43$ N/mm^2, the following equation is obtained:

$$ {}^{C}_{2mm}Q_{sky} / {}_{b}Q_{sky} = 0.432\sigma_0 + 0.649 \tag{32} $$

5.2 Comparison of calculated and experimental values

Figure 11 shows a comparison between the calculated and experimental values. The calculated values were able to accurately evaluate the experimental values. The δ_{peak} of the cylindrical shear-key under individual use is about 0.2 mm, while δ_{Hy} is 0.53 mm under combined use; thus, the δ_{peak} of the cylindrical shear-key under combined use shifts to about 0.5 mm. Considering these effects, the design value can be used as the calculated value multiplied by 0.8.

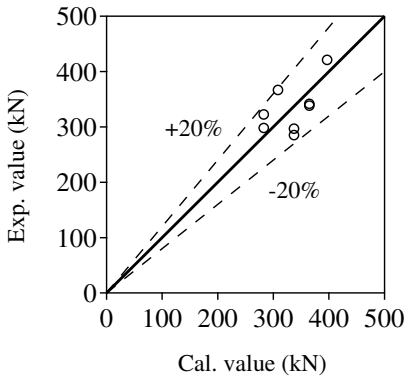

Figure 11 Comparison between the calculated and experimental values

6. Conclusion

In this study, a shear test was performed on a specimen using both a cylindrical shear-key and a post-installed anchor, the stress states due to axial stress on the joint surface were estimated from the test results, and the mechanical behavior examined in further detail. As a result, it was possible to evaluate the experimental values erring on the side of caution from the calculated values using the shear strength formula under combined use, reflecting these effects. Further findings of the study are presented below:

1) The aperture displacement δ_V of the post-installed anchor was about 1/10 of shear displacement δ_H, but δ_V under combined use generally laid in the range from 1/10 to 1/2 of δ_H;

2) Tensile strength T of the anchor bolt when used in combination was higher than under individual use, and the bending moment M was lower. From this T value, it was estimated that the shear force borne by the post-installed anchor under combined use, ${}^{C}{}_{\delta}Q_a$, was about 0.7 times that of the shear force borne by the post-installed anchor under individual use, ${}_{\delta}Q_a$;

3) Regarding the shear strength of the cylindrical shear-key under combined use, from the balance of stresses on the joint surface, the average compressive stress of the joint surface was calculated by adding 0.60 N/mm^2;

4) The calculated values were able to accurately evaluate the experimental values. The design value can be used as the calculated value multiplied by 0.8.

7. References

[1] Musha, U., Takase, Y., Abe, T., Sakamoto, K., Hiwatashi, T. and Katori, K. (2019): Supported Strength Formula of Roughened Concrete Using Shape Measurement Value by 3D-Scanner, *Journal of Technology and Design*, Architectural Institute of Japan, Vol.25, No.59, pp.55-60, 2019.2

[2] Abe, T., Hiwatashi, T., Takase, Y. and Katori, K. (2019): Mechanical Model of Cylindrical Shear-key Applied to Seismic Retrofitted Joint of Concrete Structure, *Concrete Journal*, Japan Concrete Institute, Vol.30, pp.11-20, 2019.7.

[3] Abe, T., Hiwatashi, T., Takase, Y. and Katori, K.: Mechanical Model of Post-installed Anchor Considered of Behavior of Concrete and Grout Using Reaction Modulus, *JCI Annual Convention Proceedings*, Japan Concrete Institute, No.2, pp.970-984, 2018.6

[4] Japan Building Disaster Prevention Association (2002): External Seismic Retrofitting Manual, Japan

[5] Takase, Y., Abe, T., Itadani, H., Satou, T., Kubota, M. and Ikeda, T. (2014): Estimation Method of Horizontal Capacity of Joint Fracture for Retrofitted Frame Using Disk Shear-key, *Journal of Structural and Construction Engineering*, Architectural Institute of Japan, Vol.79, No.698, pp.507-515, 2014.4

[6] Abe, T., Hiwatashi, T., Kubota, M., Takase, Y. and Katori, K. (2017): Development and Equation for Shear Strength of Cylindrical Shear-key Applied Seismic Retrofitted Joint of Concrete Structure, *Journal of Structural and Construction Engineering*, Architectural Institute of Japan, Vol.82, No.736, pp.873-883, 2017.6

[7] Takase, Y., Wada, T., Ikeda, T., Shinohara, Y. and Mizoguchi, M. (2017): Mechanical Behavior and Work of Adhesive Post-installed Anchors Subjected to Cyclic Shear Force and Constant Tensile Force, *Journal of Structural and Construction Engineering*, Architectural Institute of Japan, Vol.82, No.738, pp.1255-1263, 2017.8

